CST010

Numerical Heat Transfer of Turbulent Tube Flow through Inclined Ribs

Somchai Sripattanapipat[1], Pongjet Promvonge [2,*] and Chinaruk Thianpong[2]

[1]Department of Mechanical Engineering, Faculty of Engineering, Mahanakorn University of Technology, Bangkok 10530, Thailand
[2]Department of Mechanical Engineering, Faculty of Engineering, King Mongkut's Institute of Technology Ladkrabang, Bangkok 10520, Thailand
[*] Corresponding Author: kppongje@kmitl.ac.th, +662 329-8350, +662 329-8351

Abstract

The paper deals with a numerical study on heat transfer and flow characteristics in a heat exchanger tube with 45° inclined ribs (IR) placed periodically on two opposite tube walls. Water as the test fluid flows into the ribbed tube having a constant wall temperature condition for Reynolds numbers (Re) from 3000 to 18,000. The computations are based on the finite volume method with the SIMPLE algorithm for handling the pressure-velocity coupling. The numerical result reveals that the presence of the IR can generate a pair of main counter-rotating vortices which help induce impingement/attachment flows over the rib and some tube wall regions leading to drastic increase in the heat transfer rate. In addition, effects of rib parameters such as relative rib height (e/D) and relative rib pitch (PR=P/D) on flow resistance and thermal characteristics are numerically examined. The study shows that the heat transfer and friction loss increase considerably with the increment of e/D but the reduction of PR. The application of the IR provides higher thermal performance than the circular tube alone.

Keywords: Numerical study; Heat transfer; Inclined ribs; Turbulent flow

1. Introduction

A high-efficiency and low-resistance tubular heat exchanger is required in many industrial applications and this leads to the design and development of heat transfer enhancement techniques. Therefore, to reach the target several design features have been offered over many years, such as dimpled tubes, grooved tubes, corrugated tubes, ribbed tubes, and various tube inserts, such as twisted tape, helical screw tape, and wire coil. Ribs as a popular enhancement device are often employed in many compact heat exchangers to enhance the heat transfer rate because of their high thermal performance. Several rib configurations have been introduced in the literature [1-4] since the use of ribs can induce vortex flows (both transverse and longitudinal vortices) through the heat exchanger tubes. In general, the longitudinal vortex is found to help increase effectively heat transfer rate than the transverse vortex flow. This is why most ribs found in the literature must be inclined or angled placements instead of transverse ribs to produce longitudinal vortex. The longitudinal vortex can be steadily maintained for a long distance along the main stream under the pressure gradient by several ribs placed repeatedly along tubes/ducts. A vortex pair provide better thermal performance than a mono one.

A longitudinal vortex generator (LVG) technique has also been applied inside channels for decades. Fiebig et al. [5,6] experimentally studied the effects of the height, installed angle, number and arrangement of the LVG and showed a 50% increase in the heat transfer rate and a 45% increase in the pressure drop.

The vortex structure and temperature distribution in rectangular channels fitted with LVGs was visualized and measured by Biswas and Mitra [7]. They reported that the heat transfer was strongly enhanced and the eddy axis of longitudinal vortex was parallel to the main flow, and there existed reciprocity between different vortices, leading to excellent heat transfer performance from using the LVG. However, it is difficult to be realized inside tubes for the widely-used shell-tube exchangers. In the present work, the numerical computations for three dimensional turbulent tube flows through the 45° inclined ribs (IR) are conducted with the main aim being to examine the changes in the flow structure and heat transfer behaviors inside.

2. Tube Flow Configuration

The flow system of interest is characterized by inclined ribs placed on the tube surface as depicted in Fig 1. The flow under consideration is expected to attain a periodic flow condition in which the velocity field repeats itself from one module to another. The concept of periodically fully developed flow and it solution procedure has been described in Ref. [8]. The water entered the test tube at inlet temperature, T_{in} = 300 K. The geometrical parameters for the inclined-ribbed tube were the tube inner diameter (D) of 0.02 m, the rib width (W) of 0.001 m, and an attack angle (α) of 45° whereas e and P were the respective rib height and pitch. In the present work, the relative rib height, e/D, and relative rib pitch, PR=P/D, were varied in a range of 0.025-0.1 and 0.5-1.0, respectively.

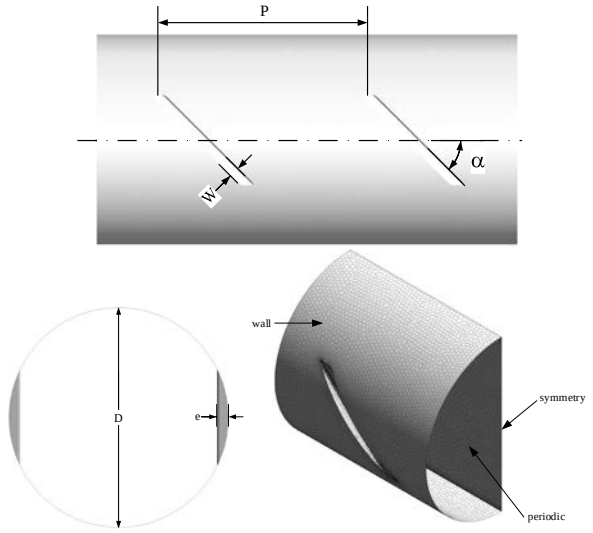

Fig. 1. Tube geometry and computational domain

3. Computational details

The numerical model for fluid flow and heat transfer in the IR tube is developed under the following assumptions: steady three-dimensional turbulent and incompressible flow and heat transfer; constant fluid properties; and neglecting viscous dissipation, body forces and radiation heat transfer.

Based on the above assumptions, the tube flow is governed by the Reynolds averaged Navier-Stokes (RANS) equations and the energy equation. In the Cartesian tensor system these equations can be written as follows:

Continuity equation:

$$\frac{\partial}{\partial x_i}(\rho u_i) = 0 \tag{1}$$

Momentum equation:

$$\frac{\partial}{\partial x_j}(\rho u_i u_i) = -\frac{\partial p}{\partial x_i} + \frac{\partial}{\partial x_j}\left[\mu\left(\frac{\partial u_i}{\partial x_j} + \frac{\partial u_j}{\partial x_i}\right) - \rho\overline{u_i' u_j'}\right] \tag{2}$$

where ρ is the density of fluid, and u_i is a mean component of velocity in the direction x_i , p is the pressure, μ is the dynamic viscosity, and u' is a fluctuating component of velocity. Repeated indices indicate summation from one to three for 3-dimensional problems.

Energy equation:

$$\frac{\partial}{\partial x_j}(\rho u_i T) = \frac{\partial}{\partial x_j}\left((\Gamma + \Gamma_t)\frac{\partial T}{\partial x_j}\right) \tag{3}$$

where Γ and Γ_t are molecular thermal diffusivity and turbulent thermal diffusivity, respectively and are given by

$$\Gamma = \frac{\mu}{\mathrm{Pr}}, \text{ and } \Gamma_t = \frac{\mu_t}{\mathrm{Pr}_t} \tag{4}$$

The Reynolds-averaged approach to turbulence modeling requires that the Reynolds stresses, $-\rho\overline{u_i' u_j'}$ in Eq. (2) needs to be modeled. The Boussinesq hypothesis relates the Reynolds stresses to the mean velocity gradients as seen in the equation below:

$$-\rho\overline{u_i' u_j'} = \mu_t\left(\frac{\partial u_i}{\partial u_j} + \frac{\partial u_j}{\partial u_i}\right) - \frac{2}{3}\left(\rho k + \mu_t \frac{\partial u_i}{\partial x_i}\right)\delta_{ij} \tag{5}$$

where k is the turbulent kinetic energy, defined by $k = 1/2 \cdot \overline{u_i' u_i'}$ and δ_{ij} is a Kronecker delta. The merit of the Boussinesq approach is the relatively low computational cost associated with the computation of the turbulent viscosity, μ_t given as $\mu_t = \rho C_\mu k^2/\varepsilon$. The RNG k–ε model is one of the two-equation models that employ the Boussinesq hypothesis.

The steady state transport equations are expressed as:

$$\frac{\partial}{\partial x_i}(\rho k u_i) = \frac{\partial}{\partial x_j}\left(\alpha_k \mu_{eff}\frac{\partial k}{\partial x_j}\right) + G_k - \rho\varepsilon \tag{6}$$

$$\frac{\partial}{\partial x_i}(\rho \varepsilon u_i) = \frac{\partial}{\partial x_j}\left(\alpha_\varepsilon \mu_{eff}\frac{\partial \varepsilon}{\partial x_j}\right) + C_{1\varepsilon}\frac{\varepsilon}{k}G_k - C_{2\varepsilon}\rho\frac{\varepsilon^2}{k} - R_\varepsilon \tag{7}$$

In the above equations, α_k and α_ε are the inverse effective Prandtl numbers for k and ε, respectively. $C_{1\varepsilon}$ and $C_{2\varepsilon}$ are constants. The effective viscosity μ_{eff} is written by

$$\mu_{eff} = \mu + \mu_t = \mu + \rho C_\mu \frac{k^2}{\varepsilon} \tag{8}$$

where C_μ is a constant and set to 0.0845, derived using the ‘‘renormalization group” (RNG) method.

All the governing equations were discretized by the QUICK numerical scheme, coupling with the SIMPLE algorithm and solved using a finite volume approach [9]. For closure of the equations, the RNG k-ε model was used in the present study. The boundary conditions are as follows: no slip and constant temperature for rib surfaces and tube walls. The periodically fully developed condition was used for the inlet and outlet section while symmetry was used for the left half-tube section as depicted in Fig. 1. The solutions were converged when the normalized residual values were less than 10^{-5} for all variables but less than 10^{-9} only for the energy equation. More details on grid independence test, boundary conditions and model validation are similar to the baffled duct in Ref. [10] and will not be repeated here for brevity.

There are three parameters of interest in the present work, namely, Reynolds number (Re), friction factor (*f*) and Nusselt number (Nu). The Re is defined as

$$\mathrm{Re} = \frac{\rho \bar{u} D}{\mu} \tag{9}$$

The f is computed by pressure drop, Δp across the tube length, L as

$$f = \frac{(\Delta p/L)D}{(1/2)\rho \bar{u}^2} \tag{10}$$

The local heat transfer is measured by local Nusselt number which can be written as

$$Nu_x = \frac{h_x D}{\lambda} \tag{11}$$

where λ is the thermal conductivity of water.

The area-average Nu can be obtained by

$$Nu = \frac{1}{A}\int Nu_x \partial A \qquad (12)$$

The thermal enhancement factor (TEF) is defined as the ratio of the heat transfer coefficient of an augmented surface, h to that of a smooth surface, h_0, at an equal pumping power and given by

$$\text{TEF} = \frac{Nu / Nu_0}{(f / f_0)^{1/3}} \qquad (13)$$

in which Nu_0 and f_0 stand for Nusselt number and friction factor for the smooth tube, respectively.

4. Results and Discussion

4.1 Validation

The comparison between the present numerical and experimental results taken from [11] are, respectively, shown in Fig. 2a and b for Nusselt number and friction factor. It is evident that the numerical results agree well with measurements for both the Nusselt number and friction factor. Quantitatively, the maximum deviations between the calculated results and experimental data were about 5% for Nu and 15% for *f*. Therefore, the present numerical predictions for heat transfer and pressure drop are judged to be reliable.

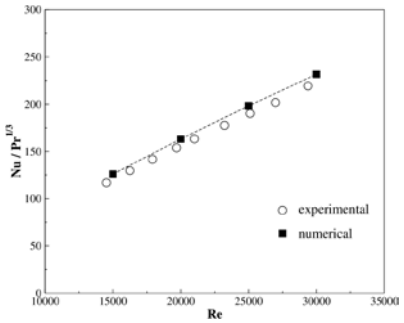

(a)

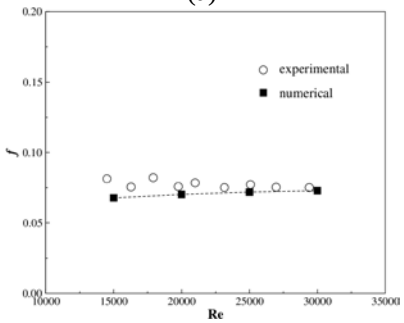

(b)

Fig. 2. Validation of (a) Nu and (b) *f*

4.2 Flow structure and heat transfer

Figure 3a, b and c displays velocity vector, streamlines and temperature contours in transverse planes at e/D=0.05, PR=1.0 and Re=12,000, respectively. The figure shows that there are two counter-rotating vortices on left and right half-sides as seen in Fig 3b. The flow structure of the two-vortices is mainly caused by the IR and is the major reason accounting for the enhancement of the heat transfer.

The temperature contour plot in transverse plane for the IR at e/D=0.05, PR=1.0 and Re=12,000 is depicted in Fig. 3c. The temperature field in the IR tube is changed dramatically by the longitudinal vortex. The temperature gradients are higher where the velocity flow toward the tube wall, while in the bottom zone of the tube where the velocity flow away from the wall, the temperature gradients are smaller.

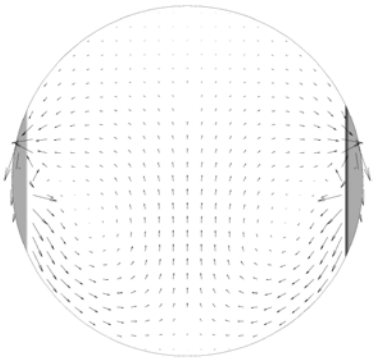

(a)

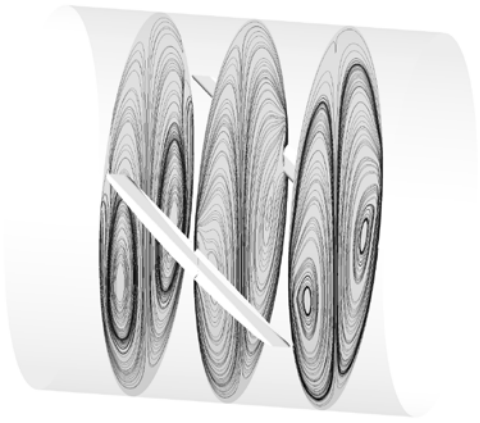

(b)

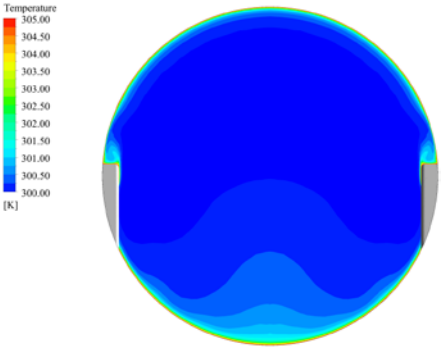

(c)

Fig. 3. (a) Velocity vector, (b) streamlines and (c) temperature contours in transverse plane, e/D=0.05, PR=1.0 and Re=12,000.

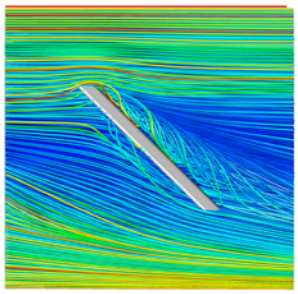

(a)

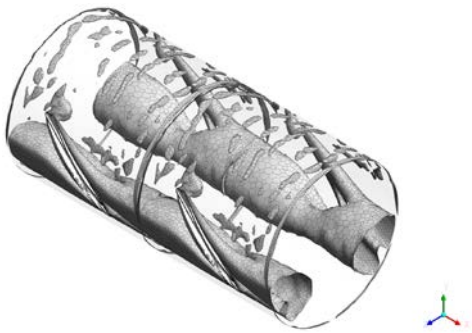

(b)

Fig. 4. (a) Streamlines around IR and (b) iso-surfaces of Q=94 for e/D=0.05, PR=1.0 and Re=12,000.

Figure 4a depicts streamlines around the IR. It is seen that there are two vortices in the vicinity of the IR. One is the front vortex appearing in the front of the IR and the other is the rear vortex behind the IR. The rear vortex has a significant effect on the heat transfer on the tube surface.

For visualization of vortices in three-dimensional flows, the coherent structure detecting method based on the Q-criterion is introduced in the current study. A rotating structure can be raised to view as an "iso-surface" of constant Q, where Q > 0 is realized. The direction of the eye or center of the vortex flow can be visualized by considering the iso-surfaces of Q = 94 as can be seen in Fig. 4b. In the figure, it can be observed that in each module, the vortex core flow is found behind the leading end of the IR before moving across the rib cavity to the rib trailing end along the sidewall to merge the upstream vortex core flow. It is concluded that the presence of the 45° IR in inline arrangement creates two main counter-rotating vortices resulting in impingement and longer flow including high strength of vortex due to changing in its orientation.

The local Nu_x contour on the tube wall for e/D=0.05, PR=1.0 at Re=12,000 is presented in Fig 5. In the figure, it appears that the high Nu is seen in the vicinity of rib surface, owing to the direct flow impingement toward to the rib surface. The Nu is also found to be relatively higher at the rear of the ribs. This is attributed to the longitudinal vortices are close to the surface and result in a fluid flow towards the tube surface and is the major reason accounting for the enhancement of heat transfer.

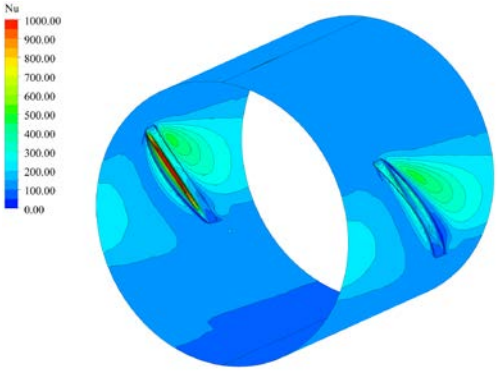

Fig. 5. Nusselt number contours at rib surface and tube wall, e/D=0.05, PR=1.00, Re=12,000.

4.3 Effect of rib height

The variation of the average Nu/Nu_0 ratio with Re for the IR tube at various e/D values is depicted in Fig 6a. The Nu/Nu_0 value tends to decrease with increasing Re but with increasing e/D. The maximum of Nu/Nu_0 is about 3.23 for e/D=0.1 and Re=3000. In general, the heat transfer augmentation is concerned with penalty in terms of increased friction coefficient resulting in higher pressure drop. Fig 6b presents the variation of the normalized friction factor, f/f_0 with Re values for e/D=0.025, 0.05, 0.075, and 0.1. In the figure, it is noted that the f/f_0 displays the uptrend with increasing the e/D. The maximum f/f_0 is 4.53 at e/D=0.1 and Re=8000.

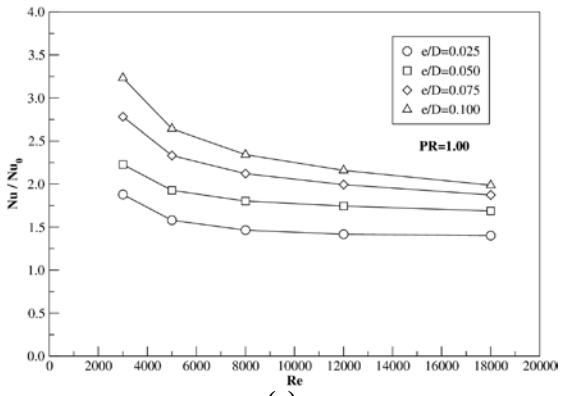

(a)

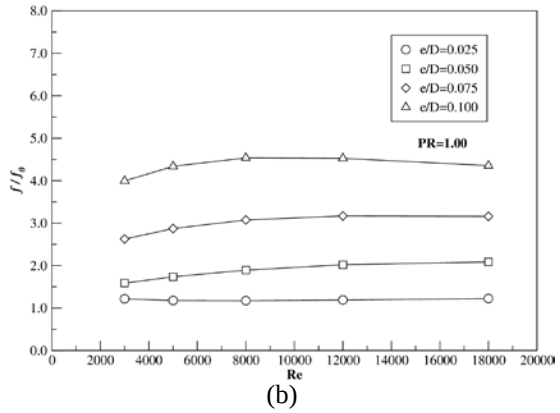

(b)

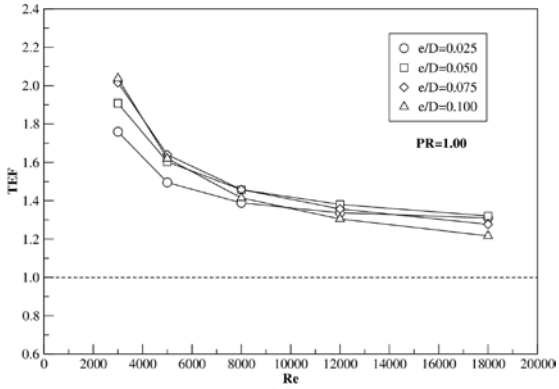

(c)

Fig. 6. Variation of (a) Nu/Nu_0, (b) f/f_0 and (c) TEF with Re at PR=1.0

Figure 6c shows the variation of thermal enhancement factor (TEF) for water flowing in the IR tube. In the figure, the TEF of the IR tends to decrease with the rise in Re. It is found that the IR tube at e/D=0.1 provides the highest TEF of 2.04. The TEF is seen to vary between 1.22 and 2.04, depending on e/D and Re values.

4.4 Effect of rib pitch

The variation of the average Nu/Nu_0 ratio with Re for the IR tube at three different PR values is depicted in Fig. 7a. The Nu/Nu_0 tends to decrease with increasing Re but with increasing PR. The maximum Nu/Nu_0 is around 2.65 for PR=0.5 at Re=3000. In general, the heat transfer augmentation is associated with pressure drop penalty in terms of increased friction factor resulting in very high pressure drop. Fig 7b presents the variation of the normalized friction factor, f/f_0 with Re values for the IR tube with PR=0.5, 0.75, and 1.0. In the figure, it is noted that the f/f_0 tends to decrease with increasing the PR. The maximum f/f_0 is 2.75 at PR=0.5 and Re=18,000.

The variation of TEF for the IR tube with various PR values is displayed in Fig. 7c. In the figure, the TEF of the IR tube shows the downtrend with the rise in Re. The highest TEF is about 2.05 for the tube with PR=0.5. The TEF is found to vary between 1.31 and 2.05, depending on PR and Re values.

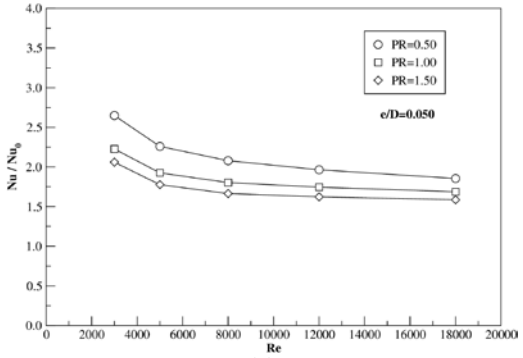

(a)

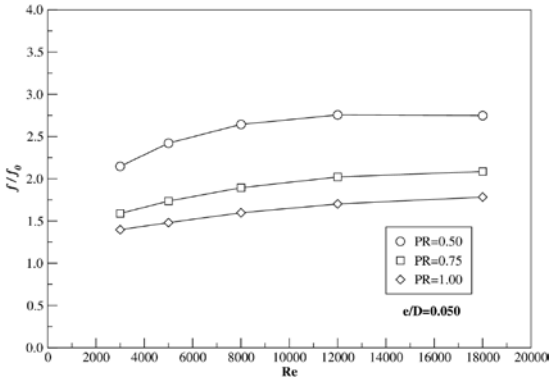

(b)

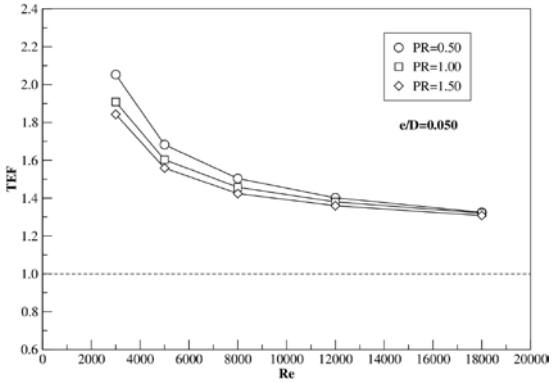

(c)

Fig. 7. Variation of (a) Nu/Nu_0, (b) f/f_0 and (c) TEF with Re at e/D=0.05.

5. Conclusions

Turbulent flow and thermal characteristics in the inclined-ribbed tube are investigated numerically. The pair-vortex flow caused by the IR helps to induce impingement/attachment flows over the tube wall leading to greater increase in the heat transfer rate. The heat transfer in the tube is about 1.40 to 3.23 times above the smooth tube. However, the heat transfer augmentation is related to the enlarged friction loss ranging from 1.17 to 4.54 times higher than the smooth tube. Thermal enhancement factor for the IR tube is higher than unity and its maximum value is about 2.05 at e/D=0.05, PR=0.5 and Re=3000, indicating higher performance over the smooth tube.

6. References

[1] Webb, R., Narayanamurthy, R., and Thors, P. (2000). Heat transfer and friction characteristics of internal helical-rib roughness, *J. Heat Transf*, vol. 122, pp. 134-142.

[2] Pal, S. and Saha, S.K. (2015). Laminar fluid flow and heat transfer through a circular tube having spiral ribs and twisted tapes, *Exp. Therm. Fluid Sci.*, vol. 60, pp. 173-181.

[3] Wang, L. and Sunden, B. (2004). An experimental investigation of heat transfer and fluid flow in a

rectangular duct with broken V-shaped ribs, *Exp. Heat. Transf.*, vol. 17, pp. 243-259.
[4] Meng, J.A., Liang, X.G. and Li, Z.X. (2005). Field synergy optimization and enhanced heat transfer by multi-longitudinal vortexes flow in tube, *Int. J. Heat Mass Transf.*, vol. 48, pp. 3331-3337.
[5] Fiebig, M., Kallweit, P., Mitra, N. and Tiggelbeck, S. (1991). Heat transfer enhancement and drag by longitudinal vortex generators in channel flow, *Exp. Thermal Fluid Sci*., vol. 4, pp. 103–114.
[6] Fiebig, M. (1998). Vortices, generators and heat transfer, *Trans. ICHemE*, vol. 76, pp. 108–172.
[7] Biswas, G. and Mitra, N.K. (1998). Longitudinal vortex generators for enhancement of transfer in heat exchanger applications, in: *11th IHTC*, Kyongju, Korea, vol. 5, pp. 334–339.
[8] Patankar, S.V., Liu, C.H. and Sparrow, E.M. (1977). Fully developed flow and heat transfer in ducts having streamwise-periodic variations of cross-sectional area, *ASME J. Heat Transfer*, vol. 99, pp. 180–186.
[9] Versteeg H.K. and Malalasekera W. (1995). An Introduction to Computational Fluid Dynamics: The Finite Volume Method, Longman Scientific & Technical, Longman Group Limited.
[10] Promvonge, P., Changcharoen, W, Kwankaomeng, S. and Thianpong C. (2011). Numerical heat transfer study of turbulent square-duct flow through inline V-shaped discrete ribs, *Int. Commun. Heat Mass Transf.*, vol. 38, pp. 1392–1399.
[11] Li, X.W., Meng, J.A. and Guo, Z.Y. (2009). Turbulent flow and heat transfer in discrete double inclined ribs tube, *Int. J. Heat and Mass Transf.*, vol. 52, pp. 962-970.